AD-785 602

INITIATION AND PROPAGATION OF LASER SUPPORTED COMBUSTION WAVES

Frank J. Allen, et al

Ballistic Research Laboratories
Aberdeen Proving Ground, Maryland

1974

AD 785 602

D D C
OCT 4 1974
F

INITIATION AND PROPAGATION OF LASER SUPPORTED COMBUSTION WAVES

FRANK J. ALLEN, WILLIAM F. BRAERMAN, CHARLES R. STUMPFEL
U. S. ARMY BALLISTIC RESEARCH LABORATORIES
ABERDEEN PROVING GROUND, MARYLAND 21005

I. INTRODUCTION

During the past few years there has been much discussion of absorption waves produced by intense laser irradiation of targets (1-6). These have been classified according to the following table (5).

Table 1. Classes of Absorption Waves

Phenomenon	Intensity (Approx.)	Propagation Velocity (Approx.)
Breakdown Wave	10^9 W/cm^2	--
Radiation Front	10^9	10^6 cm/sec
Laser Supported Detonation Wave	10^7	10^5
Laser Supported Combustion Wave	10^4	10^3
Plasmatron	10^4	0

In each case the absorption of laser beam energy behind the wave front supplies the energy required to overcome losses associated with propagation. In a detonation wave propagation is supersonic; in a combustion wave, subsonic. An optical plasmatron is a limiting case of a laser supported combustion (LSC) wave in which the laser beam intensity is just at threshold to maintain the wave stationary. Once formed an absorption wave absorbs all or a large fraction of the incident radiation, thereby shielding the target. It is therefore important to determine the conditions under which absorption waves are ignited. In this paper we will be interested in LSC waves, which occur at rather low incident intensities, and we will be interested in their ignition and propagation at sea level atmospheric pressure.

DISTRIBUTION STATEMENT A

Approved for public release;
Distribution Unlimited

16

II. CHARACTERIZATION OF LASER SUPPORTED COMBUSTION (LSC) WAVES

Most investigations of LSC (and other absorption) waves have been carried out with laboratory lasers. However, we are interested in the properties of LSC waves under field conditions where the target areas irradiated are much larger than those in the laboratory. Since the incident intensities are comparable, some information obtained in the laboratory is applicable to the field situation. Because opportunities for performing field experiments have been quite limited, and control over beam quality not completely satisfactory we make use of laboratory results to the extent practicable. We have used two high power lasers (HPL No. 1 and HPL No. 2) to produce large scale LSC waves and have used the Ballistic Research Laboratories 2 KW laser and the United Aircraft Research Laboratories (UARL) 6 KW laser in our laboratory investigations. All of these lasers operate CW at a wavelength of 10.6 µm.

We can best characterize LSC waves by first describing the experimental observations.

HPL NO. 1 EXPERIMENTAL RESULTS. Following are the principal observations concerning LSC waves produced with this laser:

1. There is a bright luminous region ∿ 100 cm long and 10 to 15 cm in diameter. Some internal structure is discernible on the film records. In particular, there is a much smaller central region which is much brighter than the remainder of the luminous region. This is the region of intersection of the laser beam with the luminous volume. The length of the brightest region, the LSC wave proper, is a few centimeters. Spectroradiometer results also attest to the fact that the strongly radiating region is a few centimeters long; in addition, we have noted that the shadows formed of nearby objects are sharp indicating that the main portion of the LSC wave radiant emission emanates from a small region.

2. Each LSC wave has its highest velocity when first distinguishable on the framing camera records. (With the instrumentation available for these experiments, the first involving large scale LSC wave behavior, LSC waves could not be distinguished from the surrounding luminous region until they had propagated a considerable distance from the target; that the LSC waves formed much nearer to the surface was clearly proven, however, by spectroradiometer data.) The propagation velocity decays approximately linearly with distance. The LSC wave peters out, i.e., ceases to be luminous, when the propagation velocity has decayed to ∿ 1 m/sec.

3. The luminous region behind the wave front has a small upward acceleration.

4. After an LSC wave forms, action--greatly reduced--continues at the same location on the target.

5. The luminous region has sharply defined boundaries. Its structure does not change rapidly; substantial changes occur over periods of tens of milliseconds.

6. Burning particles are invariably present.

7. No LSC waves formed when an airflow over the target was provided; however, the lowest airspeed used was Mach 0.1.

In these experiments intensities were in the range of 20 - 40 KW/cm^2 for the most part. LSC waves were formed with aluminum and molybdenum targets at intensities of 20 KW/cm^2; they were not formed with titanium at this intensity, nor in boron or rubber at 25 - 30 KW/cm^2, nor in tungsten at 40 KW/cm^2. An LSC wave was formed in tungsten (during a power excursion of the laser) at an intensity of 90 KW/cm^2. However, the intensities quoted are only accurate to ± 50% owing to inaccuracies both in beam power and irradiated area. Also, the number of irradiations was small, so that definitive conclusions regarding ignition threshold cannot be obtained from these results.

HPL NO. 2 EXPERIMENTAL RESULTS. Since the early experiments we have enjoyed an additional limited opportunity to produce large scale LSC waves. We designed new apparatus for studying LSC wave behavior for the latter experiments. Figure 1 shows schematically a system used to obtain time, space, and wavelength resolved spectra of LSC wave emission on each frame of a framing camera record. In addition, we arranged narrow band pass filters that permitted simultaneous transmission of LSC wave emitted light in two narrow wavelength regions to a framing camera film. This enabled us to distinguish among the several sources of light emission in the LSC wave. It enabled us to separate target vapor emission from air emission and to learn something of the transition from a target vapor dominated LSC wave to an air LSC wave.

Additional observations concerning LSC wave characteristics obtained with the aid of the equipment just described are as follows:

1. The LSC wave forms at or very near the target in a mixture of target vapor, particles, and air. No air spectra are seen

initially. Some spectra seen in the case of a 2024 aluminum target, for example, are: several Al and Mg lines, NaD lines, and AlO bands.

2. Air spectra are first seen at distances varying between 1 cm from the target surface and 10 to 12 cm depending upon the laser beam intensity.

3. The H_α line at 6563 Å, owing to water vapor in the air, is an indicator of the transition from a target vapor to an air LSC wave. This transition takes place over a small spatial region during a time of several milliseconds; it takes place on the lower edge of the LSC wave (the laser beam being horizontal).

4. Air spectra always include O, N, and H lines; N^+ lines are seen sometimes, apparently only at the highest intensities reached in the experiments, and only near the wave front.

5. The LSC waves upon occasion split into two or three distinct pieces which sometimes separate by more than one meter; this behavior is associated with the spatial structure of the beam.

6. The threshold for ignition of an LSC wave in aluminum, the material for which we have the largest body of results, is approximately the same as found in the earlier experiments, 20 KW/cm^2.

Some variation from the above general behavior is contained in the experimental results, probably caused by variations in details of the laser beam behavior. Table 2 summarizes typical characteristics of the spectral results. Figure 2 depicts the behavior in a specific case.

III. PHYSICAL PHENOMENA INVOLVED IN LSC WAVE BEHAVIOR

Guided by the experimental observations, we now wish to provide a description of the physical phenomena involved in LSC wave behavior and, in the following section, a more tentative description of the very important, more complicated initiation mechanisms, concerning which few experimental observations exist.

LSC WAVE TEMPERATURE. After formation an LSC wave is in pressure equilibrium with the surrounding air. Thus, except for minor perturbations, the pressure may be taken as one atmosphere. This, along with the temperature to be calculated, determines the degree of ionization; the latter coupled with the temperature and pressure determines the absorption coefficient for the impinging laser beam. Since, according to experiment, the laser beam is absorbed over a

ALLEN, BRAERMAN, & STUMPFEL

distance of a few centimeters we can determine a range within which
the temperature must lie. Specifically, the relationship connecting
the degree of ionization, α, absorption coefficient, K_ν, pressure, p,
and temperature, T, is

$$\alpha^2 = \frac{(T/10^4)^{7/2} K_\nu}{10.4 \, p^2 \, g} \quad , \tag{1}$$

g being approximately constant ($= 2.3$) over the temperature range of
interest (4). This equation, with p and g fixed as stated, and α a
tabulated function for air (7,8), is readily solved for assumed
values of K_ν, which must be in the range of 0.1 to 0.7 to be in
accord with the observed absorption in the experiments. Solving
Eq. (1) under these conditions, we obtain temperatures in the range
11,500 to 15,200 $^{\circ}$K.

For the case of air seeded with target vapor we cannot use
the tabulated properties of air. Instead we use the Saha equation
for (single) ionization equilibrium. However, since the degree of
target vapor ionization is large we have modified the usual form of
this equation (6). The calculation of LSC wave temperature proceeds
in the same fashion for this case except that we must now assume
values for the molar concentration of target vapor. So doing, we
find that the temperature, in the case of an aluminum target, lies
between 6000 and 8000 $^{\circ}$K. (Aluminum vapor provides almost all of the
ionization, air a small amount, because aluminum has a much lower
ionization potential than any of the constituents of air.)

The calculated temperature ranges are consistent with
several experimental observations. First, for a given temperature
and LSC wave volume, we obtain the power radiated from calculated
curves which have been checked against experiment in the range of
interest (9). We find that most of the power absorbed from the laser
beam is reradiated. Next, we have calculated spectra emitted by air
at temperatures of interest from results of Biberman et al. (10),
modified to account for geometrical differences. We find that:

1. The radiating volume is "thin"; i.e., almost all of the
emitted radiation escapes the hot plasma except for that emitted at
wavelengths shorter than approximately 1100 $\overset{\circ}{A}$.

2. The spectral distribution of the radiation is consis-
tent with spectroradiometer results (measured power radiated in
selected wavelength intervals) for an air LSC wave in the 12,000 to
15,000 $^{\circ}$K range and for a target vapor seeded LSC wave $\sim$ 7000 $^{\circ}$K.

3. An estimate of the total power radiated based on the calculated spectral distribution is consistent with that calculated from the spectroradiometer data, assuming the spectral distribution to be correct (which is consistent with the results already mentioned).

4. For some of the LSC waves observed in the experiments N^+ spectral lines were seen at times near the wavefront (oscillating on and off, owing to laser power fluctuations); for other LSC waves no N^+ spectra were seen. This, taken in conjunction with known air species concentrations as functions of temperature, suggest that the lower and higher LSC wave temperatures are $\sim$ 12,000 and 14,000 ^{O}K, respectively (9,11).

5. The temperatures deduced are in the general range observed in more carefully controlled laboratory experiments in which the intensities were comparable while the spot sizes were much smaller and the observed radiation source was the limiting case of an LSC wave, a plasmatron. Using the BRL 2 KW laser (in argon) a temperature of 13,000 ^{O}K has been obtained. Using the UARL 6 KW laser (in air) a temperature of 17,000 ^{O}K has been obtained.

POWER BALANCE. Having determined the relevant temperature range, we can make a power balance in the LSC wave. We have shown that the power radiated constitutes the major portion of that absorbed from the laser beam. For a given temperature we can calculate the stored energy, which turns out to be quite small. (There is also stored energy in the luminous region surrounding the LSC wave, the luminosity being caused by metastable species. We have estimated the density of this region from its rate of rise in the earth's gravitational field; this, and the fact that it is at atmospheric pressure, determine its average temperature, $\sim$ 700 ^{O}K, and its energy content, which turns out to be quite small.) Since the structure of the wave has been observed to change rather slowly, changes in stored energy have a negligible effect on the power balance. Likewise, calculation of the thermal conductivity of air at the relevant temperatures, and consideration of the dimensions of the LSC waves, show that heat conduction plays only a minor role (6).

Finally, there is a transfer of energy by convection; we cannot estimate this accurately. We obtain a rough estimate by calculating the rate of air engulfment by the LSC wave using experimentally observed dimensions (cross-sectional areas) and propagation velocities, and multiplying this result by the energy gain per unit volume of cold air entering the wave. We find that convective power transfer is not small; however, it is not as large as the power radiated.

PROPAGATION VELOCITY. The final characteristic of an LSC wave (after initiation) which we wish to discuss is its propagation velocity. This, we have observed, decays essentially linearly with distance. Raizer's theory (4) provides an expression for the velocity dependent upon the beam intensity (which varies as the wave propagates toward the laser since the beam is focused). However, this theory is applicable only to small scale LSC waves where heat conduction rather than radiation dominates the energy transfer processes. Application of Raizer's theory to the present LSC wave data results in velocities much smaller than those observed. We wish to emphasize, however, that the propagation velocity is only partially determined by coupled radiation and hydrodynamics: a very essential ingredient is the initial mass and velocity of the hot gas. This is associated with the initiation mechanisms to be discussed in the next section. Briefly, the vapor (and particles) which blow off the target and first form an absorbing region, receive a velocity directed from the target toward the laser in the blowoff process. The mass removed from the target and the time to form an absorbing region depend in some fashion upon beam intensity and target material; (for large beams the area irradiated is probably not important.) In addition, as the absorbing region forms and heats, there is an exodus of gas from the volume (to maintain pressure equilibrium with the surroundings); the interaction of the ejected gas with the target results in additional momentum of the material in the absorbing region, directed away from the target. This effect can be quite large according to (one dimensional) calculations by Hall et al. (11). The dimensions of the initial absorbing region, for a given target material, can vary considerably with incident intensity; according to our most recent experimental observations of LSC waves, in which we placed two narrow band pass filters in parallel in front of a lens and framing camera, the transition from a target vapor to an air LSC wave may take place within 1 or 2 cms of the target or may occur 10 or 12 cms away from the target (for an aluminum target).

The observed, approximately linear, velocity decay is then partly caused by the sharing of momentum with engulfed air and partly caused by diminution in beam intensity as the LSC wave progresses toward the laser. (The latter need not always be true: by focusing the beam in front of the target, the LSC wave can be made to propagate into a region of increasing beam intensity; we have done this but, owing to inadequate control over beam quality. no definitive results have been obtained as yet.) The observed velocity decay rates of the LSC waves support the above statements as we have shown by intercomparing decay rates for LSC waves in air formed with different target materials (6). Except for propagation velocity all of the characteristics of an LSC wave, after the transition from

target vapor to air has been made, are determined solely by the properties of air, the target vapor being too dilute to play a role once the air has been ionized significantly.

IV. MECHANISMS OF INITIATION

Initiation of an LSC wave takes place in some mixture of target vapor, burning target particles, and air. The transition to an LSC wave in air usually occurs within 1 or 2 cms of the target surface; however, when the laser beam intensity is barely sufficient to support an LSC wave in air, the transition may occur up to 10 or 12 cms from the target. In some cases the transition fails to occur, the LSC wave petering out as the target vapor becomes more dilute.

A target vapor-air mixture at the boiling point of most metals does not have a sufficient degree of ionization to absorb the laser beam significantly, thereby become hotter. Consider, for example, the case of aluminum whose boiling point is 2720 $^\circ$K. Pure aluminum vapor at atmospheric pressure does not significantly absorb a 10.6 μm wavelength laser beam below a temperature of approximately 5000 $^\circ$K (12); the mixtures of aluminum vapor and air we previously considered absorbed the laser beam, over the observed distances, at temperatures in the 6000 - 8000 $^\circ$K range. We are therefore led to a search for processes which can lead to heating of the electrons (after which these electrons can cause impact ionization resulting in a rate of gain of electrons which exceeds the loss rate; i.e., a cascade process occurs, the medium then becoming capable of absorbing the incident laser beam).

Many mechanisms have been considered for intensities of 10^7 W/cm^2 or higher (13). The levels of interest here are $\sim 10^4$ to 10^5 W/cm^2. At the higher intensities the transient pressure at the target surface can be much greater than atmospheric with the result that the temperature can greatly exceed the normal boiling point; the thermionically emitted electrons are then characterized by a much higher temperature and give rise to impact ionization. Walters (13) has considered various suggested mechanisms which play a role in this higher intensity regime. All of the suggested mechanisms appear to be applicable only at intensities much higher than those of present concern. On the other hand the role of particles blown off the target, of which a great many are experimentally observed, has not been considered. (We have demonstrated (6) that the small particles keep up with the LSC wave as it forms and moves away from the target.) That the hot burning particles play a role seems clear since they are in the vapor-air mixture where initiation occurs while, as we have seen, initiation does not occur at the target surface.

As is the case at the target surface, there appears to be no way the pressure at the surface of a small particle can be raised sufficiently to increase the particle's boiling point significantly (in spite of the large surface tension such particles possess): a very high pressure is required to raise the temperature appreciably while, because of its small volume (hence mass) to area ratio, a small pressure gradient within the particle will cause its disintegration. Such disintegrations are commonly seen in metal flames (14,15) and appear to occur even more readily when the burning takes place in a laser beam (16). Thus the electrons thermionically emitted from the particles do not possess the requisite high temperature. (Their density can be high within a few particle radii; escape to greater distances is prevented by image charges developed on the particles.)

COMBUSTION OF METALS. Most metals have high heats of combustion which lead to high adiabatic flame temperatures, usually $\sim$ 2000 to 4000 °K; the actual flame temperature is lower owing to losses (17). For example, aluminum has an adiabatic flame temperature of approximately 3900 °K (18). There has been a great deal of study of the burning of small metal particles as this is of much practical interest from several standpoints. The oxidation mechanisms of various metals differ depending on many thermophysical and mechanical properties of both the metals and their oxides (15). Again taking aluminum as an example, an Al_2O_3 shell forms outside the oxidizing particle; oxidation of the vapor emitted by the enclosed boiling aluminum takes place at the surface of the oxide layer (18). In this case the flame temperature cannot exceed the oxide boiling point of 3800 °K since the oxide decomposes upon vaporization, as it does for most metal oxides (17). (A layer of AlO gas can conceivably form outside the molten Al_2O_3 shell, and this highly absorbs 10.6 μm radiation as do some other metal oxides; however, the surrounding vapor has a high thermal diffusivity, and therefore a large diffusion length, even on a msec time scale. A simple calculation shows that the heat capacity of the vapor, which must be heated along with the absorbing AlO gas, is large enough so that the temperature rise is negligible.)

We believe that a clue as to the means by which high electron temperatures come about is to be found in the behavior of metal flames without the presence of a laser beam. It is well known that electron temperatures can greatly exceed the gas temperature and that electron densities can be orders of magnitude greater than their equilibrium density (19). A plausible explanation for this has been given by Von Engel (19): During the oxidation process, products of reaction are formed in excited states. Electrons

undergo collisions with the excited reaction products, part of the excitation energy being converted to kinetic energy of motion of the electrons. This is illustrated by the reaction

$$A^* + e_{slow} \rightarrow A + e_{fast} \qquad (2)$$

where A, e are an atom (or molecule) and electron, respectively, and the asterisk indicates an excited state. Making use of the principal of detailed balance, Von Engel has calculated cross sections for several such processes and obtains fairly large values in cases involving electronic excitation.

While inverse reactions occur, the flow of chemical energy (i.e., the heat of combustion) results in a net transfer of energy to the electrons causing their mean energy or the electron temperature to be higher than that of the neutral gas. While Von Engel's illustrative calculations do not apply directly to metal-oxident reactions, it is well known that such reactions are among the brightest chemiluminescent reactions (20). The radiation from such reactions emanates from electronically excited atoms and molecules populated directly by chemical reactions.

The effect of the laser beam's impinging on the oxidizing particles must be to increase the temperature of the entire system (it increases the flame temperature by counteracting heat losses): The absorption of infrared radiation by small particles is generally broadband (21) in contrast to absorption in molecular band systems. This absorption is high even for a "good conductor" such as aluminum--at the high temperatures in question all of the metals have high resistivities.

MATERIAL DEPENDENCE. Most of the LSC waves studied have been produced with metallic targets. We noted in the Introduction, however, that we did not ignite LSC waves in boron or rubber at intensities sufficient for ignition in aluminum and molybdenum. Likewise Fowler et al. (12) have ignited LSC waves in many metals with a 6 KW CO_2 CW laser (at intensities of 10^6 to 10^7 W/cm^2--higher than those of concern here, yet lower than the intensities at which target plasma properties rather than properties of the solid target are dominant); they failed to ignite wood or plexiglas at the highest intensity they were able to achieve, twice that required to ignite metals. These materials have low flame temperatures. Pyroceram, composed of several metallic oxides, ignited LSC waves with the same intensities as required by the metals. The vaporization temperature of pyroceram is $\sim$ 2000 to 3000 $^\circ$K. The possibility exists that the metallic oxides decompose, then reoxidize at a later stage in the process,

26

ALLEN, BRAERMAN, & STUMPFEL

forming reaction products in excited states. This could lead to
heating of thermionically emitted electrons followed by ignition as
described above. (In all cases the reaction products remaining in
the LSC wave after formation are dissociated into their constituent
atoms, absorbing energy in the process—this after they have been
instrumental in igniting the LSC wave; we note also that at high
temperatures thermionic emission from insulators can be high (22)
owing to the large decrease in the bandgap.)

CONVERSION TO AIR LSC WAVE. Finally, the conversion of the LSC wave
in the target vapor-particle-air mixture to an LSC wave in air
probably takes place in a straightforward manner. The energy absorbed
by the LSC wave is transferred to the engulfed air as the wave propa-
gates and the target vapor becomes progressively more dilute. The
transition occurs on the lower edge of the wave (for a horizontal
beam). air flowing into the wave mainly at the bottom as material
from the target vapor-air mixture rises.

V. SUMMARY AND CONCLUSIONS

The principal experimental findings and the conclusions
based upon a description of the physical processes which at least
qualitatively explain all of the experimental results are:

1. LSC waves in air form anywhere from 1 cm to 10 or 12 cm
from the target surface depending upon beam intensity and target
material. Typical dimensions of the most intense emission region
are: 2 to 3 cm diameter; 3 to 4 cm length.

2. The absorbing region is first formed in a mixture of
target vapor, particles, and air.

3. Burning particles play a major role in LSC wave
ignition at incident intensities of 10^4 to 10^5 W/cm^2. In the oxida-
tion reactions electronically excited products form and transfer
energy to electrons thus causing an electron temperature substan-
tially higher than the gas temperature. Cascade ionization follows,
the electrons giving rise to impact ionization at a rate exceeding
the electron loss rate. Details are specific to each target material,
though some similarity in the behavior of various metals is to be
expected.

4. Metals and some metallic compounds ignite LSC waves at
least somewhat more readily than do other materials that have been
tried. A low ionization potential material favors ignition.

5. An LSC wave receives initial momentum directed away from the target the magnitude of which depends upon incident intensity and target material.

6. The LSC wave when first formed in the target vapor-air mixture has a temperature generally in the range of 6000 - 8000 °K. The target vapor seeds the air and supplies almost all of the ionization.

7. After the transition from an LSC wave in the target vapor-air mixture to an LSC wave in air, the temperature reaches the 12,000 - 14,000 °K range.

8. The air LSC wave radiates a considerable amount of energy in the vacuum ultraviolet wavelength region of the spectrum. This radiation is to a considerable extent absorbed in the surrounding cold air and plays a role in LSC wave propagation.

9. After formation the LSC wave absorbs a large fraction, in some cases almost all, of the incident laser beam, thus cutting the beam off from the target. When one LSC wave peters out--after reaching a low velocity ambient air currents coupled with diminished beam intensity result in insufficient power to sustain it--another forms near the target, provided the beam characteristics have not changed. Note: No LSC waves have been formed in the few experiments in which we provided air flow over the target. However, the lowest air speed we used in the experiments was Mach 0.1.

REFERENCES

1. Yu. P. Raizer, Soviet Physics JETP 21, 5 (1965).

2. Yu. P. Raizer, Zh ETF Pis' ma 7, 2 (1968).

3. F. V. Bunkin, V. I. Konov, A. M. Prokhorov, and V. B. Fedorov, Zh ETF Pis' Red. 9, 11 (1969).

4. Yu. P. Raizer, Soviet Physics JETP 31, 6 (1970).

5. P. E. Nielsen and G. H. Canavan, AFWL Laser Digest, Dec. 1971.

6. F. J. Allen, O. R. Lyman, J. C. Barb, K. Frank, and C. R. Stumpfel, BRL Report No. 1643, April 1973. (Secret).

7. A. S. Predvoditelev, E. V. Stupochenko, E. V. Samuilov, I. P. Stakhanov, A. S. Pleshanov, and I. B. Rozhdestvenskii, Tables of Thermodynamic Functions of Air for the Temperature Range 6000 - 12,000 °K and Pressure Range 0.001 - 1000 atm., Infosearch Limited, London, 1958.

8. J. Hilsenrath, AEDC TN 56-12, Addendum.

9. J. W. Bond, Jr., K. M. Watson, and J. A. Welch, Jr., Atomic Theory of Gas Dynamics, Addison-Wesley, Reading, Massachusetts, 1965.

10. I. V. Avilova, L. M. Biberman, V. S. Vorobjev, V. M. Zamalin, G. A. Kobzev, A. N. Lagar'kov, A. Ch. Mnatsakanian, and G. E. Norman, J. Quant. Spectrosc. Radiat. Transfer 9, 1969, pp. 89-122 and Tables, pp. 1285-1312. (Articles in Russian).

11. R. B. Hall, W. E. Maher, and P. S. P. Wei, AFWL-TR-73-28, June 1973.

12. M. C. Fowler, D. C. Smith, C. O. Brown, and R. J. Radley, Jr., ∪ARL Report N921716-7, Jan. 1974, ARPA Order No. 2113.

13. C. T. Walters and R. H. Barnes, Battelle Columbus Laboratories, Nov. 1973, ARPA Order No. 2113.

14. R. Friedman and A. Macek, Combustion and Flame 6, 1962, pp. 9-19.

15. T. A. Brzustowski and I. Glassman, Progress in Astronautics and Aeronautics, Vol. 15, 1964, pp. 41-74.

16. I. Liebman, J. Corry, and H. E. Perlee, Combustion Science and Technology 5, 1972, pp. 21-30.

17. A. V. Grosse and J. B. Conway, I and EC, 50, 4, 1958.

18. R. W. Bartlett, J. N. Ong, Jr., W. M. Fassell, Jr., and C. A. Papp, Combustion and Flame 7, 1963, pp. 227-234.

19. A. Von Engel, Brit. J. Appl. Phys. 18, 1967, pp. 1661-1677.

20. S. E. Johnson, P. B. Scott, G. Watson, Xonics, Inc., Final Rept., Contr. No. DAAH01-73-C-0548.

21. H. C. Van de Hulst, Light Scattering by Small Particles, John Wiley and Sons, Inc., New York, 1957.

22. S. L. Soo, J. Appl. Phys. 34, 6 (1963).

Table 2. Spectral Observations

Spot Size	Strongest Observed Spectra	Physical Interpretation	Remarks
3-12 cm	AlO Molecular bands; Strong Al lines; impurity lines (Na and Mg)	Vaporization of aluminum; chemical combustion of Al vapor and particles	Emission often extends many cms from target
2-6	Very strong Al line emission and Na, Mg line emission	Vaporization; excitation of Al (and impurities)	Emission extends a few cms from target; many KW of power radiated in visible region
2-4	N, H, O lines and occasional N+ lines	Ionization of the air	LSC wave propagates away from target

Aluminum target   Laser beam power $\approx$ 130 KW
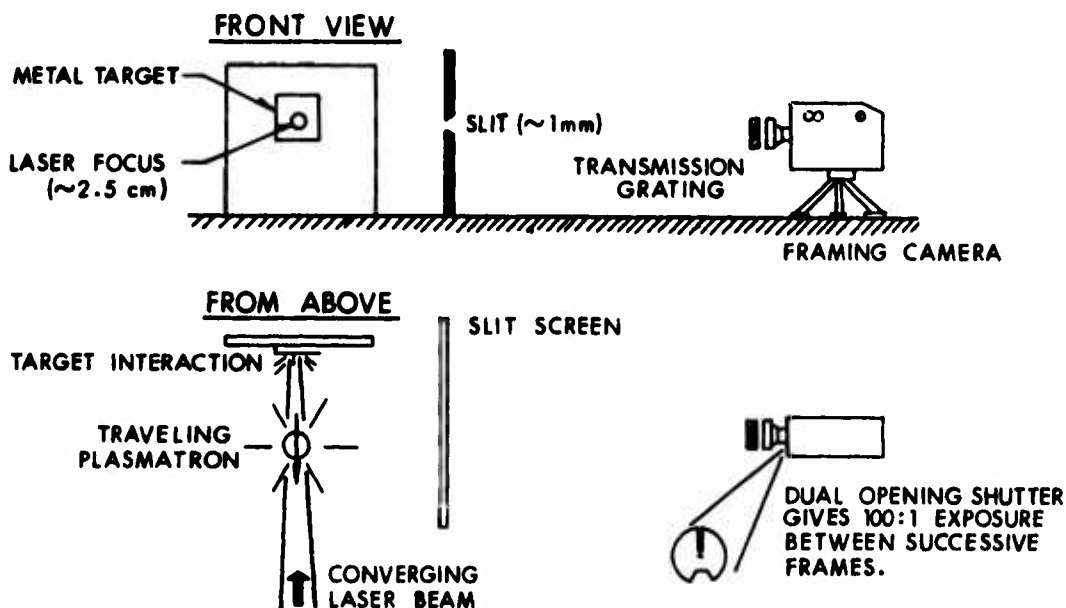
Fig. 1.   Transmission Grating Measurement of LSC Wave Emission.
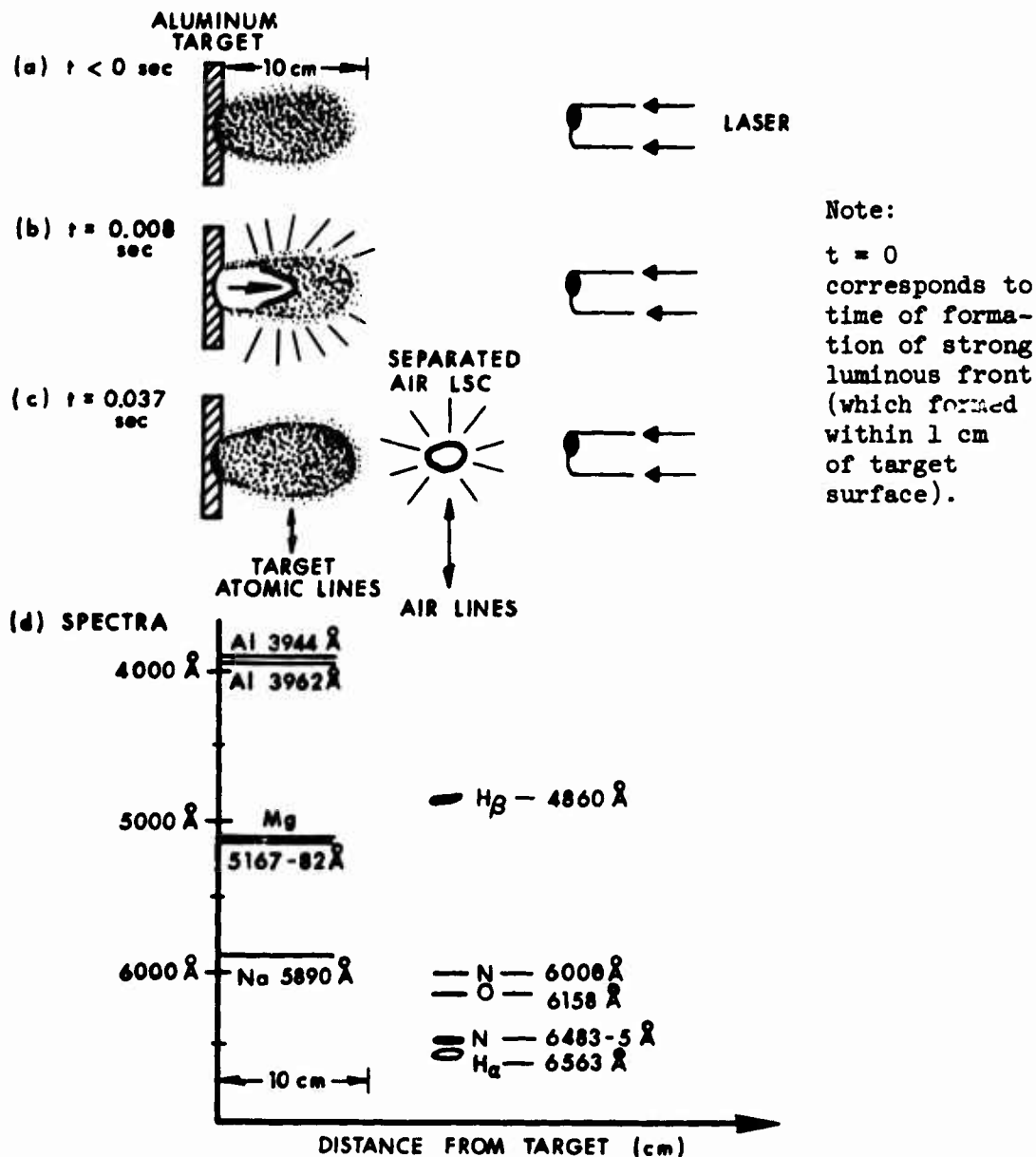
Fig. 2. Sketches of Sequence of Events Leading to LSC Wave Formation and Propagation. (a) Luminous target vapor and oxide particles. (b) Strong luminous front 0.008 sec after formation. (c) Strongly radiating air LSC wave separated from target vapor. (d) Spectra corresponding to (c); strongest emission lines are shown and serve to distinguish between air and target vapor dominated behavior.